Original article

MOLECULAR METABOLISM

Excessive exercise elicits poly (ADP-ribose) Polymerase-1 activation and global protein PARylation driving muscle dysfunction and performance impairment

Barbara M. Crisol[1], Matheus B. Rocha[1], Beatriz Franco[2], Ana Paula Morelli[1], Carlos K. Katashima[1], Scylas J.A. Junior[1], Fernanda S. Carneiro[1], Renata R. Braga[1], Rafael S. Brícola[1], Graciana de Azambuja[2], Raul Gobato Costa[3], Andrea M. Esteves[2], Marcelo A. Mori[3], Maria C.G. Oliveira[2], Dennys E. Cintra[4,5], José R. Pauli[1,2,5], Filip J. Larsen[6], Adelino S.R. da Silva[7,8], Eduardo R. Ropelle[1,2,5,*]

ABSTRACT

Excessive exercise combined with inadequate recovery time may trigger fatigue, performance impairment, and ultimately the overtraining syndrome. The intramyocellular mechanisms involved in the overtraining syndrome remain only partially known. Here, we combined multi-omics analyses from isogenic BXD mouse strains with a mouse model of overtraining and excessive exercise protocol in mice and humans to evaluate the molecular mechanism involved in the performance impairment induced by excessive exercise. We identified that BXD mouse strains with elevated levels of *Parp1* gene expression in the skeletal muscle displayed features like overtraining syndrome and abnormal muscle genetic signature. High PARP1 protein content and aberrant PARylation of proteins were detected in the skeletal muscle of overtrained, but not in trained mice. Overtraining syndrome reduced mitochondrial function promoted by exercise training, induced muscle hyperalgesia, reduced muscle fiber size and promoted a similar gene signature of myopathy and atrophy models. Short periods of excessive exercise also increased PARylation in the skeletal muscle of mice and healthy subjects. The pharmacological inhibition of PARP1, using Olaparib, and genetic *Parp1* ablation, preserved muscle fiber morphology and protected against physical performance impairment and other symptoms of the overtraining syndrome in mice. In conclusion, PARP1 excessive activation is related to muscle abnormalities led by long or short periods of excessive exercise, and here we suggest that PARP1 is a potential target in the treatment and prevention of overtraining syndrome.

Keywords Exercise; Muscle; PARP1; overtraining

1. INTRODUCTION

Excessive physical exercise without sufficient recovery time typically leads to muscle damage, performance stagnation, or decline, which can have serious consequences for both athletes and non-athletes. These effects include fatigue, metabolic disorders, immunological and hormonal alteration, as well as psychological disturbances [1—4]. This condition is known as non-functional overreaching (NFOR), which takes weeks or months for full recovery, whereas the overtraining syndrome requires even more time [1—4]. Although these are systemic conditions, skeletal muscle metabolism plays a critical role in the etiology of NFOR and overtraining syndrome [5—7]. Excessive exercise induces muscle damage, inflammation, oxidative stress, abnormal mitochondrial function, and reduced glycogen content. These skeletal muscle alterations are often associated with low oxidative capacity, muscle weakness, pain, and performance worsening [5,8—10]. However, unfortunately, there is no specific therapy to prevent or treat skeletal muscle disorders associated with the NFOR and the overtraining syndrome.

Recently, Poly (ADP-Ribose) Polymerase-1 (PARP1) activation has emerged as a critical target for skeletal muscle metabolism and function, under physiological and pathological conditions [11—17]. PARP1 acts as a DNA damage sensor and is highly expressed across the tissues of mammals, including in the skeletal muscle. PARP1 post-transcriptionally controls its targets through the ADP-ribosylation process, which consists of the sequential ADP-riboside attachments

[1]Laboratory of Molecular Biology of Exercise (LaBMEx), School of Applied Sciences, University of Campinas (UNICAMP), Limeira, SP, 13484-350, Brazil [2]School of Applied Sciences, University of Campinas, Limeira, SP, Brazil [3]Department of Biochemistry and Tissue Biology, Institute of Biology, University of Campinas (UNICAMP), Brazil [4]Laboratory of Nutritional Genomic, School of Applied Sciences, University of Campinas (UNICAMP), Limeira, SP, 13484-350, Brazil [5]Obesity and Comorbidities Research Center, University of Campinas (UNICAMP), Brazil [6]The Swedish School of Sport and Health Sciences, GIH, Åstrand Laboratory, Department of Physiology, Nutrition and Biomechanics, Stockholm, 114 33, Sweden [7]Postgraduate Program in Rehabilitation and Functional Performance, Ribeirão Preto Medical School, University of São Paulo (USP), Ribeirão Preto, SP, Brazil [8]School of Physical Education and Sport of Ribeirão Preto, University of São Paulo, Ribeirão Preto, SP, Brazil

*Corresponding author. University of Campinas Laboratory of Molecular Biology of Exercise, 13484-350, Limeira, SP, Brazil. E-mail: eduardoropelle@gmail.com (E.R. Ropelle).

Received December 30, 2024 • Revision received March 27, 2025 • Accepted March 29, 2025 • Available online 3 April 2025

https://doi.org/10.1016/j.molmet.2025.102135

on target proteins triggering the poly (ADP-ribose) (PAR) formation, this mechanism is also known as, PARylation [18]. PARP1 activation governs several biological processes such as repair and DNA replication, cell cycle control, apoptosis, inflammation, and others [18,19]. Strikingly, skeletal muscle-specific PARP1 knockdown increased resistance to oxidative stress, mitochondrial biogenesis, climbing ability, and extended lifespan in *Drosophila* [15]. Furthermore, pharmacological PARP inhibitors reversed mitochondrial defects in primary myotubes of obese humans [16]. In this context, we hypothesize that PARP1 could be a promising target to counteract the skeletal muscle abnormalities induced by NFOR or overtraining syndrome.

2. METHODS

2.1. BXD muscle transcriptomic and metabolomic analyses

Transcriptomic analyses were performed using skeletal muscle mRNAs of the BXD inbred family (BXD Muscle Affy Mouse Gene 1.0 ST Record: 10352242 n = 40, strains) and metabolomic analyses were performed using a muscle metabolome data set (EPFL/LISP BXD Muscle Polar Metabolites CD_Jun14). Transcripts, metabolites and phenotype data sets are accessible on GeneNetwork (http://www.genenetwork.org). Pearson's and Spearman's correlations, as well as scree plot graphs were built using PrismGraph, and the heat map graphs were obtained using the Gene-E software. The Principal Component Analysis (PCA) was originally performed in the GeneNetwork platform, and then the two factors analysis graphs were modified using CorelDRAW 2021 software, version 23.1.0.389.

2.2. Cell culture

C2C12 myoblasts were maintained in growth medium DMEM supplemented with 10% Fetal Bovine Serum (FBS) and 1% Penicillin-streptomycin. For differentiation to myotubes, cells were seeded at 5000 cells/cm^2 into plates and proliferated for 2 days to reach 90% confluency and maintained in differentiation media for 7 days (DMEM high glucose with 2% Horse Serum). All experiments were conducted after 7 days of differentiation.

Cell viability was measured using 3-[4,5-dimethylthiazol-2-yl]-2,5 diphenyl tetrazolium bromide (MTT) assay (M6494, Merck). Briefly, cells were seeded in 96 well plates and MTT was added at 10% of total volume at 5 mg/mL and incubated for 2 h at 37 °C. The absorbance was measured at 560 nm using a microplate reader machine to indicating treatment time points. Olaparib was diluted in 100% DMSO and H_2O_2 in PBS.

2.3. Mouse models

Eight-week-old male C57BL/6J mice were acquired from the University of Campinas (UNICAMP) animal facility. The *Parp1* knockout mice and its control model 129S1/SvImJ were acquired from Jackson Laboratory (stock #002779 and #002448). The animals were placed in groups of five per cage, with controlled temperature (between 20 °C and 22 °C) on a 12:12-h light–dark cycle with food and water *ad libitum*. The diet was composed of AIN-93M with protein supplementation from AIN-93G prepared at the School of Applied Sciences of UNICAMP. The experiments were approved by the ethics committee from UNICAMP, with protocol numbers 5000-1/2018, 5993-1/2022 and 6419-1/2024. The number of animals used in each experiment is specified in the figure legends.

2.4. Incremental load test

For the running performance analysis and the definition of the exercise session intensities, the mice were submitted to an incremental load test as previously described [20]. Briefly, the test starts at an initial intensity of 6 m/min, with increments 3 m/min every 3 min until exhaustion. The exhaustion was considered when the animals reached the end of the treadmill five times in 1 min gap. The peak workload was the intensity at the exhaustion point of the test.

2.5. Training and overtraining protocol

Before the experimental period, the mice were acclimated to the treadmill to minimize the possible stress induced by the equipment. The exercise training program was performed as previously described [20] (Table 1). To define the exercise intensity and exercise performance, at the beginning, after four weeks, and at the end of the experimental period, the animals underwent an incremental load test [20]. The overtraining protocol was described by Pereira et al. [21] (Table 2).

2.6. Short-term excessive exercise protocol for mice

Before the experimental period, the mice were acclimated to the treadmill. The animals were subjected to 3 consecutive days of running at 60% of the peak power until exhaustion or for a maximum period of 120 min. This first part of the protocol was named "moderate". After that, the mice were submitted to an additional 7 consecutive days of running at 60% of peak power until exhaustion or for a maximum period of 180 min (Table 3). This second part of the protocol was named "excessive". Physiological parameters and performance tests were assessed before and during the last two days of the protocol (days 9 and 10). In these two days, beyond the performance test and physiological analyses, the animals also performed the daily session of excessive exercise.

2.7. Grip test

Twenty-four hours after the final exercise session, the animals were submitted for the grip test. The animals were acclimated to the test by performing three attempts. Before the test, they rested for 5 min. Each animal underwent five attempts to measure grip strength. The best and worst results were discarded from the analyses. The results are represented by the average of the three attempts considered after the test.

2.8. Four paws strength test

Twenty-four hours after the final exercise session, the animals underwent the four-paws strength test, as previously described [22], with minor adjustments. The mice were positioned in the center of a steel

Table 1 — Exercise training protocol.

Weeks	Intensity (% peak power)	Duration (min)	Daily sessions	Treadmill grade (%)	Recovery between sessions (h)
1	60	15	1	0	24
2	60	30	1	0	24
3	60	45	1	0	24
4	60	60	1	0	24
5 to 8	60	60	1	0	24

Table 2 — Overtraining protocol.

Weeks	Intensity (% peak power)	Duration (min)	Daily sessions	Treadmill grade (%)	Recovery between sessions (h)
1 to 4	It is the same as the training protocol				
5	60	60	1	−14	24
6	70	60	1	−14	24
7	75	75	1	−14	24
8	75	75	2	−14	4

Table 3 — Short term of excessive exercise protocol.

Experimental day	Intensity (% peak power)	Duration (min)	Daily sessions	Treadmill grade (%)	Recovery between sessions (h)
1 to 3	60	120	1	0	22
4 to 8	60	180	1	0	21

screen, which was later inverted, forcing the animals to remain on the underside of the screen suspended by their four paws. The animals remained in this position until failure. Five attempts were made per animal. The longest and shortest times were discarded from the analyses, and the average of the other attempts was used as a measurement of strength resistance.

2.9. Ambulatory activity and grooming analysis

The behavior of the animals was analyzed using the activity box (locomotion) and the open field arena (grooming behavior). Records of the locomotor activity were obtained in 30 × 30 cm cages. Through a camera, the animal's movements were determined by tracking sensors. The route analyzed was divided into 16 quadrants, 4 in the central area and 12 in the peripheral area. The length of stay (seconds) in each area and the number of quadrants covered were recorded. The nature or speed of movements was not analyzed. Total locomotor activity counts were recorded over 30 min using the Arena Video Tracking-Bonther program.

The Open Field test was performed in a circular arena with a diameter of 60 cm, divided into 8 peripheral quadrants and 4 central quadrants. Each animal remained in the test for 10 min, and only the final 5 min were evaluated. The test was carried out in the presence of an evaluator, and the grooming variable (face and body washing) was analyzed using a stopwatch.

2.10. Olaparib treatment

During the overtraining experiments, mice were treated with Olaparib from Glenthan Life Science (GP0126) added to the diet at 50 mg/kg/day, as described by Gariani and colleagues [23], starting on the first day of the training protocol. For the excessive exercise protocol, the same dose of Olaparib was administered daily by intraperitoneal injection.

2.11. Mechanical muscle nociceptive threshold test

Mechanical muscle hyperalgesia was measured by the Randall-Selitto algesimeter (Insight, Brazil), which applies a linear mechanical pressure on the gastrocnemius muscle as previously published [24]. Muscle hyperalgesia was acquired by subtracting the baseline measurement from the measurement performed every week starting from week 4 of the protocol, after a rest period of 50—54 h.

2.12. Evans blue injection

Twenty hours before the euthanasia, mice were intraperitoneally injected with 1% Evans blue dye (EBD) in phosphate-buffered saline (PBS, pH 7.5) sterilized by passage through a Millex®-GP 0.22 μm filter (Millipore, Bedford, MA, USA) and stored at 4 °C [25]. The volume of EBD injected was 1% of the body weight of each animal.

2.13. Tissue sampling

Mice were euthanized by deepening anesthesia, using an intraperitoneal injection of ketamine chlorohydrate (10%) (300 mg/kg, Syntec, Cotia,SP, Brazil) and xylazine chlorohydrate (2%) (30 mg/kg, Syntec, Cotia, SP, Brazil), followed by cervical dislocation. The skeletal muscles (gastrocnemius, extensor digitorum longus/EDL, tibialis anterior), fat pads (epididymal, retroperitoneal and mesenteric) and spleen samples were weighed. Samples of the gastrocnemius muscle were extracted and snap-frozen or fresh-analyzed during mitochondrial respiration analyses.

2.14. Real-Time PCR

Total RNA was extracted from gastrocnemius of excessive training mice (20—30 mg) using TRIzol™ reagent (1 mL per sample) (#15596026, Thermo Fisher Scientific). The cDNA was synthesized using the iScript™ cDNA Synthesis Kit, (#1708891, Bio-Rad) with 1.000 ng of total RNA. The qPCR reaction was performed using iTaq Universal SYBR Green Supermix (#1725121, Bio-Rad), and the quantitative differences in mRNA expression were calculated according to the comparative threshold (Ct) cycle method using β-actin as the housekeeping gene. Samples were run in the 7500 Real-Time PCR System (Applied Biosystems; Thermo Fisher Scientific).

Primers Sequence:

*Actb*_fwd: 5′-CATTGCTGACAGGATGCAGAAGG-3';
Actb rev: 5′-TGCTGGAAGGTGGACAGTGAGG -3';
Parp1 fwd: 5′-CTCTCCCAGAACAAGGACGAAG -3';
Parp1 rev: 5′- CCGCTTTCACTTCCTCCATCTTC-3′

2.15. High-resolution respirometry (HRR)

The HRR was performed in permeabilized muscle fibers from the same portion of gastrocnemius as previously described [26]. After dissection, the muscle was cleaned and placed in an ice-cold BIOPS buffer. The muscle fiber bundles were gently separated using thin forceps and put in a 12 well plate containing 2 mL of BIOPS and 50ug/mL of Saponin at 4 °C for 30 min. After that, the muscle bundles were placed in a well containing ice-cold MIR buffer for 5—10 min. The muscle bundles were placed in a paper filter to remove the media excess and weighed. Next, 1.5 mg was put into an Oxygraph-2k chamber (Oroboros Instruments Corporation, Innsbruck, Austria) with 2 mL of MIR buffer. The respiration assay was performed by analyzing Complex I proton leak (CI_L), by adding malate and glutamate to a final concentration 0.5 mM and 10 mM, respectively, followed by maximum CI respiration capacity by adding ADP to a 5 mM final concentration.

The addition of Succinate, to a 10 mM final concentration, stimulated Complex II (CII), reflecting at this point the complex I + II phosphorylated respiration. Oligomycin, an ATP synthase inhibitor, was added in a 2.5 μM final concentration to access the non-phosphorylating resting state (Leak). After that, carbonyl cyanide-4-(trifluoromethoxy) phenylhydrazone (FCCP) was added using 0.5 μM titulation until no further increase in respiration was observed. This respiration value corresponds to maximum respiration capacity (ETS). Finally, Rotenone (0.5 μM final concentration) and Antimycin A (2.5 μM final concentration) were added to analyze residual oxygen respiration not related to mitochondria.
The results for ATP linked respiration are the values from CI + II phosphorylated activity minus the values from Olygomicin. The proton leak results are the subtraction of non-mitochondrial respiration from the Olygomicin values.

2.16. Western blotting

The fresh frozen gastrocnemius was homogenized in the extraction buffer as previously described [27]. The protein concentration in the supernatant portion of the sample was determined using the bicinchoninic acid method and Laemmli buffer was added to each of the samples. The muscle lysate was subjected to SDS-PAGE and transferred to nitrocellulose membranes that were incubated with 5% dry milk at room temperature for 60 min and then incubated in the primary antibody. The following antibodies were used: Anti-OXPHOS (mitochondrial subunits cocktail) (ab110413) from ABCAM (Cambridge, United Kingdom), anti-Hsp60 (SC-13115) from Santa Cruz Biotechnology (Santa Cruz, CA, USA), anti-LonP1 (BS4245R) from Bioss, anti-PAR (AM80) from Millipore, anti-GAPDH (#2118), anti-beta Actin (#3700), anti-PARP1 (#9542), anti-phospho-JNK (#9255E), anti-caspase 8 (#4927) and anti-caspase 9 (#9508) from Cell Signaling (Danvers, MA, USA). Next, the membranes were incubated with the specific secondary antibody, corresponding to the primary antibody. The specific bands were labeled by chemiluminescence using Signal Fire ECL reagent from Cell Signaling (Danvers, MA, USA) and were visualized using G:Box from Syngene. Ponceau staining from Sigma—Aldrich (Saint Louis, MO, USA) was utilized as a loading control reference.

2.17. Immunohistochemistry

The gastrocnemius muscle was dissected and frozen in isopentane. 10 μm cryosections were prepared using a cryostat (Leica) at −25 °C. For the muscle damage assay using Evans blue dye, the slides were dried at room temperature for around 20 min and fixed with acetone at −20 °C for 10 min. Afterward, the samples were washed with PBS at room temperature three times for 10 min each. The slices were dried and stained with DAPI.
For the morphology assay, the slices were fixed with PFA 4% for 5 min at room temperature and washed with ddH2O. Once the slices were dry, they were stained with Harris Hematoxylin for 5 min and washed with running ddH2O for 10 min. Next, the samples were stained with 0.5% eosin solution in ddH2O and acetic acid for 10 min.

2.18. Muscle fiber size analysis

For fiber size analysis, the images from hematoxylin and eosin staining were imported to CellPose (https://www.cellpose.org) to segment the fibers in the images. After segmentation, the resulting mask was imported to QuPath [28] to measure the intensity levels across these segmented fibers.

2.18.1. RNA-seq analyze

Total RNA content was isolated from gastrocnemius samples (replicates = 3 per group) using TRIzol reagent (Invitrogen, Grand Island, NY, USA) according to the protocol. LaCTAD (UNICAMP, Brazil) performed the library preparation and sequencing using Illumina NextSeq2000. The quality control of the FASTQ files was performed using the FastQCR package, and the data was trimmed using Trimmomatic and filtered low-expressed genes (<5 counts in >3 replicates). The samples were aligned using the STAR package, and the read counts were performed using the Feature Counts package. The normalization and differential expression analysis were performed using the DESeq2 package. All the data processing was performed using R studio (version 2024.4.2.764). Only significant results are shown (q-values <0.1; padj <0.05).

2.19. NAD + analyses

The gastrocnemius NAD + analyses were performed using an enzymatic coupled cycling assay as previously described [29].

2.20. Human sample analysis

The samples from human skeletal muscle analyzed in this paper were previously described by Flockhart and colleagues [30]. Samples from 7 subjects were analyzed under basal conditions after 2 weeks of High-Intensity Interval Training (HIIT), here named “moderate” and after 3 weeks of HIIT, here named “excessive”. The protein content evaluations were performed by Western blotting using the following primary antibodies: anti-PARP1 (SC-56196) and anti-HSP60 (SC-59567) from Santa Cruz Biotechnology, Inc and anti-PAR (MABE1031) from Merck Life Science. MEMCODE staining was used as the loading control.
The performance/PARylation ratio was calculated by dividing the maximal heart rate measurement during the third week of the HIIT session, by muscle PARylation levels.

2.21. Statistical analysis

All results were expressed as mean ± standard deviation (SD). Normality was assessed using a Shapiro—Wilk test. For data with the normal distribution, one-way analysis of variance (ANOVA) was used to compare more than two groups. The Tukey's or Dunnett's *post-hoc* tests were used. For non-normal distribution, the data was analyzed using the nonparametric test, Kruskal—Wallis, adopting the Trained group as the control column for multiple comparisons using Dunn's post-hoc test. When two groups were compared, the data was analyzed by paired or unpaired t-student test for normal distribution and Mann—Whitney for non-normal distribution. The normality of human data was assessed using a Shapiro—Wilk test. For a normal distribution, the data were analyzed through a one-way analysis of variance (ANOVA), followed by Dunnett's multiple comparisons test. For non-normal distribution, the Friedman test was used for analysis, with the excessive exercise group serving as the control column for multiple comparisons, followed by Dunn's post-hoc test. The outlier ROUT or Grubb's tests were performed considering Q = 1% and alpha = 0.05, respectively. Pearson's and Spearman's correlations were used for BXD analyses. All statistical analyses were performed in Graph Pad Prism 9.5.1 for Windows (Graph- Pad Software, San Diego, California, USA), and a p-value of <0.05 was considered significant.

3. RESULTS

3.1. High Parp1 gene expression in skeletal muscle reveals overtraining-like symptoms in BXD isogenic mouse strains

The multi-omics panel of the BXD mice is a powerful and accurate resource for the analysis of genome-to-phenome linkage [31,32]. This mouse genetic reference population is derived from crosses of C57BL/6J and DBA/2J inbred strains (Fig. S1A). To understand the biological relevance of the *Parp1* genetic variation in the skeletal muscle, we employed an analytical pipeline using transcriptome and metabolome data from the gastrocnemius muscle associated with wide phenotypic data.

Skeletal muscle transcriptome analysis across 40 BXD isogenic strains revealed muscle transcript signatures were affected by *Parp1* genetic variation (Fig. 1A). The heat map (Fig. 1A), multi-correlation graph (Fig. 1B) and Principal Component Analysis (PCA) (Fig. 1C) demonstrated that *Parp1* gene expression was positively associated to fibrosis/collagen-, myopathy-, DNA repair-, ubiquitin/proteasome

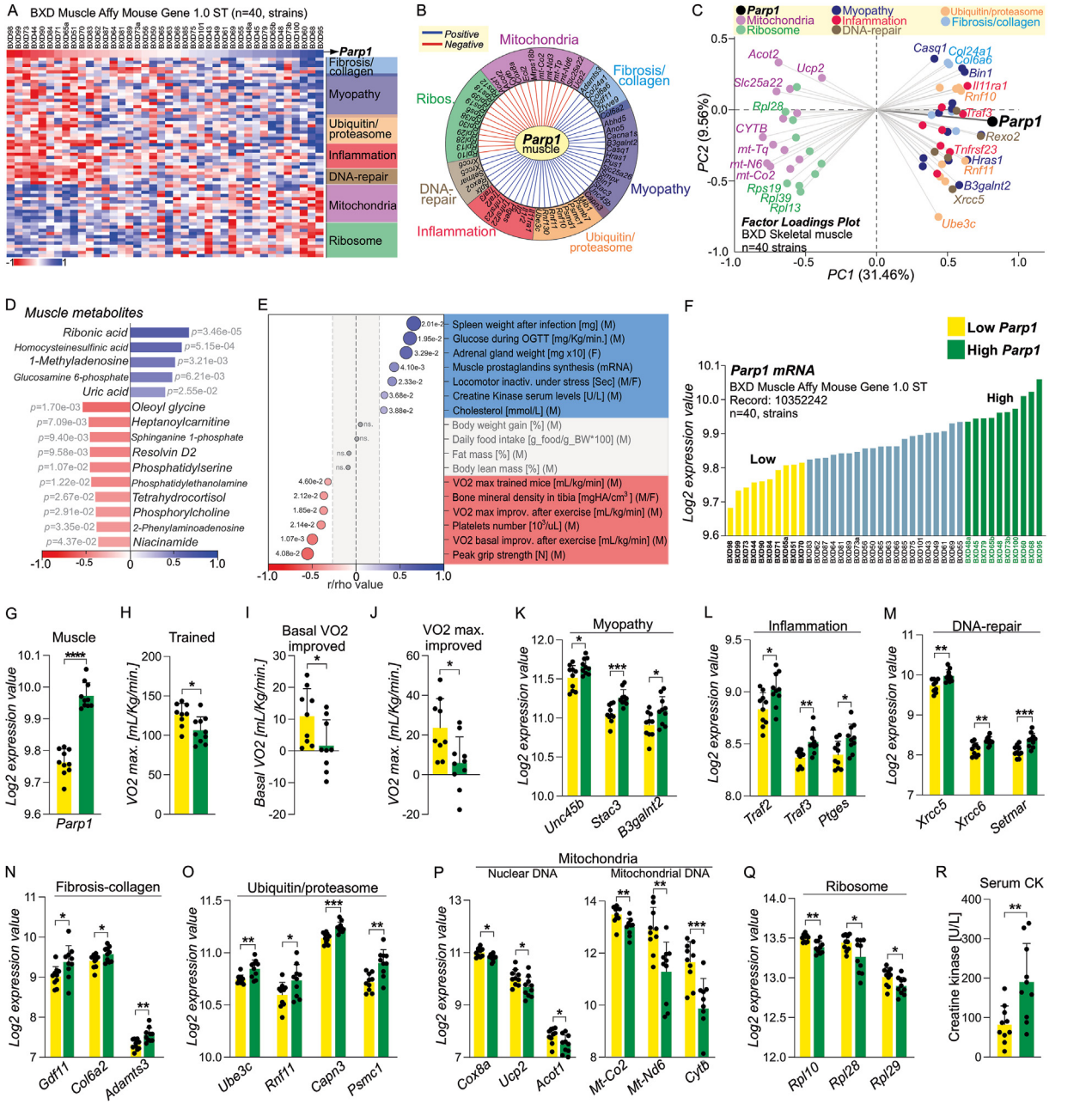

Figure 1: The overtraining-like symptoms are associated with *Parp1* gene expression in skeletal muscle. (A) Muscle transcripts from 40 BXD mouse strains. (B) Correlation graph using muscle *Parp1* mRNA and skeletal muscle transcripts from BXD strains (n = 42). (C) Principal component analysis (PCA) (n = 40). (D) Pearson's correlations between muscle *Parp1* gene expression and muscle metabolites. (E) Muscle *Parp1* expression was associated with several overtraining-like symptoms of male and female BXD mice. Pearson and Spearman's analyses were used. (F) Muscle *Parp1* expression across 40 BXD strains. (G) 10 lowest (yellow) and 10 highest (green) *Parp1* gene expression in muscle (n = 10). (H) VO_2max in trained BXD mice (n = 10). (I) Basal VO_2 improved and (J) VO_2max improved after a short period of aerobic training (n = 9–10). (K–Q) Muscle gene expression. (R) Creatine kinase serum levels. Student's *t*-test was used in G-R. *, $p < 0.05$, **, $p < 0.01$, ***, $p < 0.001$ and ****, $p < 0.0001$. (For interpretation of the references to color in this figure legend, the reader is referred to the Web version of this article.)

system- and inflammation-related genes and negatively associated to ribosome- and mitochondrion-related genes in the skeletal muscle.

The muscle metabolome analysis demonstrated that muscle *Parp1* genetic variation was strongly and positively linked with ribonic acid levels, an intermediate product from ribose metabolism [33,34], which is critical for PARP1 activity (Fig 1D). Other metabolites harmful to muscle metabolism were also found, including uric acid (Fig 1D). Conversely, metabolites involved in the inflammation resolution process (Resolvin D2 and 2-Phenylaminoadenosine) and in NAD + metabolism (i.e., niacinamide), were negatively impacted due to the *Parp1* genetic variation in the skeletal muscle (Fig 1D).

Interestingly, muscle *Parp1* transcripts were positively associated with several overtraining-like features including, immunological response markers (spleen weight, prostaglandins synthesis, and platelets number), metabolic disorders (glucose intolerance and high cholesterol levels), stress (adrenal gland hypertrophy, abnormal behavior (inactivity under stress), muscle damage marker (creatine kinase serum levels), low physical performance [maximal oxygen uptake (VO_2 max.) and strength], and low capacity to improve aerobic performance (basal and VO_2 max improvement after exercise) (Fig 1E).

Next, BXD strains were stratified following *Parp1* gene expression in the skeletal muscle, and the lowest 10 (yellow) and highest 10 (green) strains were studied (Fig. 1F). While a statistical difference was found in *Parp1* gene expression in the muscle of these selected mice (Fig. 1G), no difference was observed in the gene expression of other PARPs isoforms in the skeletal muscle (Fig. S1B). In addition, alterations of *Parp1* gene expression were observed in the gastrocnemius muscle but not in other tissues, such as the liver, heart, and adipose tissues (Figs. S1C—F). Notably, BXD mice with the highest *Parp1* gene expression in the skeletal muscle displayed lower aerobic capacity in response to physical training (Fig. 1H) and lower capacity to improve basal oxygen uptake (VO_2) and VO_2 max in response to exercise (Fig. 1I and J). Importantly, these indicators of worst performance are not related to heart mass (Fig. S1G), heart rate (Fig. S1H), intramuscular content of phospho-creatine, glycogen, ATP, or amino acid (Fig. S1I-L). However, BXD mice with the highest *Parp1* gene expression in the skeletal muscle presented unfavorable genetic signatures in muscle, showing elevated levels of genes related to myopathy, inflammation, DNA repair, collagen, fibrosis, and the ubiquitin-proteasome system (Fig. 1K-O) and suppression of mitochondrial- and ribosomal-related genes (Fig. 1P and Q). Consistent with these data, serum levels of creatine kinase were increased in BXD strains with higher *Parp1* gene expression in the skeletal muscle (Fig. 1R). These initial findings support that muscle *Parp1* genetic variation is intricately linked to several NFOR- and overtraining-like features in mice.

3.2. Overtraining induces PARP1 activation and global PARylation of proteins in the skeletal muscle of mice

To validate the genetic findings, a specific mouse model of overtraining protocol was employed [21]. A key indicator of overtraining is stagnation or a decline in performance. Previous research has shown that excessive running protocols with uphill, downhill, or no inclination result in similar performance impairments [35]. Although downhill running induces eccentric contractions, which cause muscle damage through distinct mechanisms compared to isometric or concentric contractions, Morais et al. [36] compared moderate and overtraining protocols performed downhill and found that only the latter impaired performance in mice. This finding highlights the crucial role of the imbalance between high-intensity exercise and recovery in performance decline. Given our objective to assess the extent of muscle damage associated with performance decline, we selected a downhill overtraining protocol. Mice were subjected to training or overtraining protocols for 8 weeks (Fig. 2A). Both exercise regimens produced a discrete reduction in body weight, but no statistical difference was reached (Fig. S2A). Trained and overtrained mice presented a reduction in the epididymal fat content (Fig. S2B). No difference was observed in the muscle weight (Fig. S2C). However, while regular exercise training protocol progressively improved the physical performance (Figs. S2D—F), overtraining led to impaired aerobic capacity and muscle strength when compared to the trained group (Fig. 2B and C). In addition, overtrained mice showed stress behavior (Fig. 2D) and reduced spontaneous activity by about 40% when compared to trained mice, although a statistical difference was not reached ($p = 0.0686$) (Fig. 2E).

Notably, the overtraining protocol increased both PARP1 protein content and the accumulation of PARP1 cleaved form, compared to the trained group (Fig. 2F). Consistent with this, high levels of global protein PARylation were observed in the gastrocnemius muscle of overtrained mice (Fig. 2G). This strong PARP1 activation agrees with DNA damage of muscle fibers induced by this overtraining model, as we previously reported [37].

Histological analysis showed that overtraining promoted a significant reduction in the fiber size area (Fig. 2H and I). Muscle damage was detected by Evans blue staining in overtrained mice (Fig. 2J). Cellular stress and apoptotic markers were also detected in the muscle in response to overtraining (Fig. 2G and H). A functional test for pain determination confirmed the muscle abnormalities and low nociceptive threshold in the skeletal muscle of the hindlimb of overtrained mice (Fig. S2G and H).

Overtraining also induced mitochondrial stress, as determined by the accumulation of Heat shock protein 60 (HSP60) and Lon protease homolog (LONP1), mitochondrial unfolded protein response (UPRmt) markers (Fig. S2I). High-resolution respirometry revealed that while regular training increased mitochondrial respiration capacity in the skeletal muscle, overtraining reduced it (Fig. 2L).

In addition, RNA sequencing analysis from the gastrocnemius muscle of trained versus overtrained mice was performed. A total of 44 genes were modulated, including genes related to myopathy, atrophy, collagen synthesis, inflammation, and membrane transporters (Fig. 2M, N and S2J). Collectively, these data confirmed that overtraining induces severe injury and aberrant PARP1 activation in the skeletal muscle.

3.3. Genetic and pharmacological PARP1 inhibition prevents performance impairment induced by overtraining

To understand the effects of PARP1 in the skeletal muscle during overtraining, homozygous *Parp1* global knockout (*Parp1*$^{-/-}$) and the background strain, 129S2/SVPas (129S) were studied (Fig. 3A). At the basal conditions, 129S and *Parp1*$^{-/-}$ displayed no significance in the body weight, as well as skeletal muscles, adipose, and heart weights (Fig. 3B—E). A greater cross-sectional area of the muscle fiber (Fig. 3N, left panels), by about 7.2% (Fig. 3O) of *Parp1*$^{-/-}$ mice under rest conditions, compared to the 129S group. However, no difference was found in terms of maximum power, endurance capacity, and muscle strength in these strains under sedentary conditions (Fig. 3F—H).

Next, 129S and *Parp1*$^{-/-}$ mice were subjected to the overtraining protocol (Fig 3I). Interestingly, overtraining reduced the aerobic performance in 129S but not in *Parp1*$^{-/-}$ mice, when compared to their respective trained groups (Fig. 3J). After the overtraining protocol, the grip strength was 12% higher in the *Parp1*$^{-/-}$ when compared to 129S mice (Fig. 3K). Western blotting analyses from gastrocnemius muscle demonstrated that

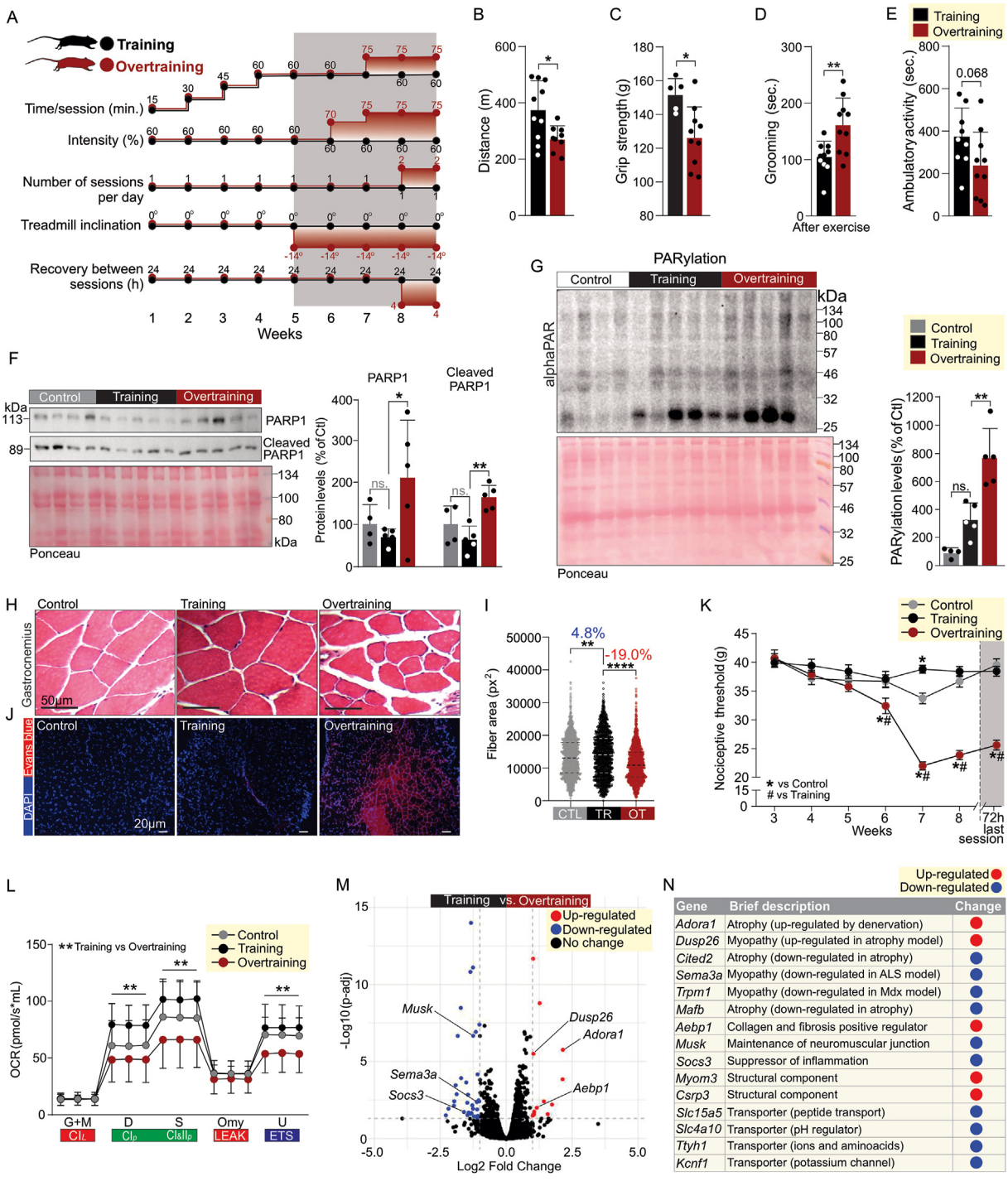

Gene	Brief description	Change
Adora1	Atrophy (up-regulated by denervation)	●
Dusp26	Myopathy (up-regulated in atrophy model)	●
Cited2	Atrophy (down-regulated in atrophy)	●
Sema3a	Myopathy (down-regulated in ALS model)	●
Trpm1	Myopathy (down-regulated in Mdx model)	●
Mafb	Atrophy (down-regulated in atrophy)	●
Aebp1	Collagen and fibrosis positive regulator	●
Musk	Maintenance of neuromuscular junction	●
Socs3	Suppressor of inflammation	●
Myom3	Structural component	●
Csrp3	Structural component	●
Slc15a5	Transporter (peptide transport)	●
Slc4a10	Transporter (pH regulator)	●
Ttyh1	Transporter (ions and aminoacids)	●
Kcnf1	Transporter (potassium channel)	●

Figure 2: Effects overtraining in the skeletal muscle of mice. (A) Experimental design. (B) Covered distance (n = 10 and 9). (C) Grip strength (n = 5 and 10). (D) Grooming and (E) ambulatory activity analysis during the open field test (n = 9–10). (F) Cleaved form of PARP1 (n = 4–5). (G) Global protein PARylation (n = 4–5). (H) Eosin and hematoxylin analysis (n = 5–6). (I) Fiber area measurement (n = 1699). (J) Evans blue staining (red) (n = 2–3). (K) Nociceptive threshold test (n = 5). (L) Mitochondrial oxygen consumption in gastrocnemius muscle (n = 8–9). (M and N) Transcriptome data from skeletal muscle of trained versus overtrained mice (n = 3). Student's *t*-test was used in B-E, and analysis of variance (ANOVA) was used in F, G, I, K, and L. *, $p < 0.05$, #, $p < 0.05$, **, $p < 0.01$, ***, $p < 0.001$ and ****, $p < 0.0001$. (For interpretation of the references to color in this figure legend, the reader is referred to the Web version of this article.)

the absence of *Parp1* protected against overtraining-induced aberrant protein global PARylation (Fig. 3L), inflammation, and mitochondrial stress (Fig. 3M). While overtraining altered the muscle morphology and reduced the cross-sectional area of the muscle fiber in 129S mice by about 7%, *Parp1*$^{-/-}$ overtrained mice displayed better muscle fiber organization and preserved the muscle fiber area when compared to 129S overtrained mice (Fig. 3N and O).

We next tested a preventive therapy model for overtraining. For this, Olaparib, an FDA-approved PARP-1 pharmacological inhibitor, was

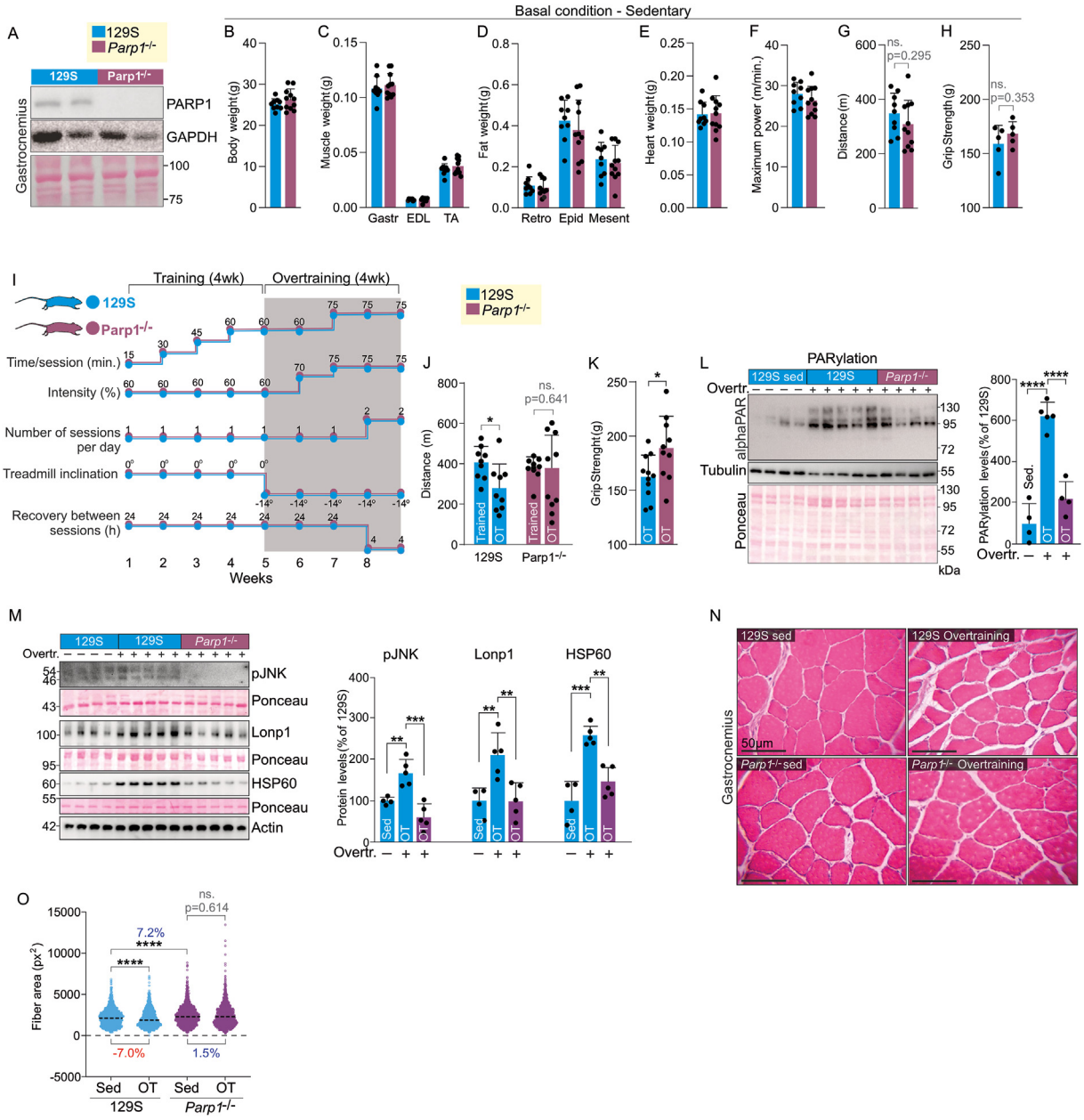

Figure 3: Effects overtraining in *Parp1*$^{-/-}$ mice. (A) Representative Western blot of PARP1 protein content in gastrocnemius muscle of 129S1/SvImJ and full *Parp1*$^{-/-}$ mice at rest. (B) Body weight, (C) muscle weights, (D) fat pad weights, (E) heart weights, (F) maximum power, and (G) covered distance in sedentary male mice (n = 9 and 11). (H) Grip strength in sedentary male mice (n = 5). (I) Experimental design of the overtraining protocol in 129S1/SvImJ and full *Parp1*$^{-/-}$ male mice. (J) Covered distance during the exhaustive test (n = 9 and 10). (K) Grip strength (n = 11 and 10). (L) Global protein PARylation in the skeletal muscle (n = 4–5). (M) JNK phosphorylation and Lonp1 and HSP60 protein content in the gastrocnemius muscle. (N) Eosin and hematoxylin analysis from gastrocnemius muscle (n = 3). (O) Fiber area measurement (n = 3007–3668). Student's *t* test was used in B–K, and analysis of variance (ANOVA) was used in L, M and O. *, $p < 0.05$, **, $p < 0.01$, ***, $p < 0.001$ and ****, $p < 0.0001$.

used. Olaparib is a potent PARP1 inhibitor (IC_{50} = 5.0) with a lower capacity to inhibit PARP2 (IC_{50} = 1.0) [38]. First, we analyzed the Olaparib effects in differentiated C2C12 myotubes exposed to hydrogen peroxide (H_2O_2), which is known to induce cellular damage. While Olaparib alone (0.5 mM) did not change cell viability (Fig. S3A), H_2O_2 promoted, as expected, a strong stressful effect on myotubes, reducing the cell viability (Fig. S3B). H_2O_2 (500 mM) also increased global protein PARylation and reduced cell viability by about 50% (Fig. S3D and E). However, Olaparib completely blocked the global protein PARylation and increased the cell viability by about 15% of myotubes exposed to H_2O_2 (Fig. S3D and E).

Afterward, preventive therapy was evaluated *in vivo* by adding daily Olaparib to the diet during the overtraining protocol in C57BL6j mice. Olaparib treatment did not change PARP1 protein content in the skeletal muscle of overtrained mice (Fig. 4A). Notably, Olaparib mitigated the aberrant global protein PARylation in the skeletal muscle of mice induced by the overtraining, keeping the PARylation levels similar to the control group (Fig. 4B). Since PARP1 is known as a NAD^+

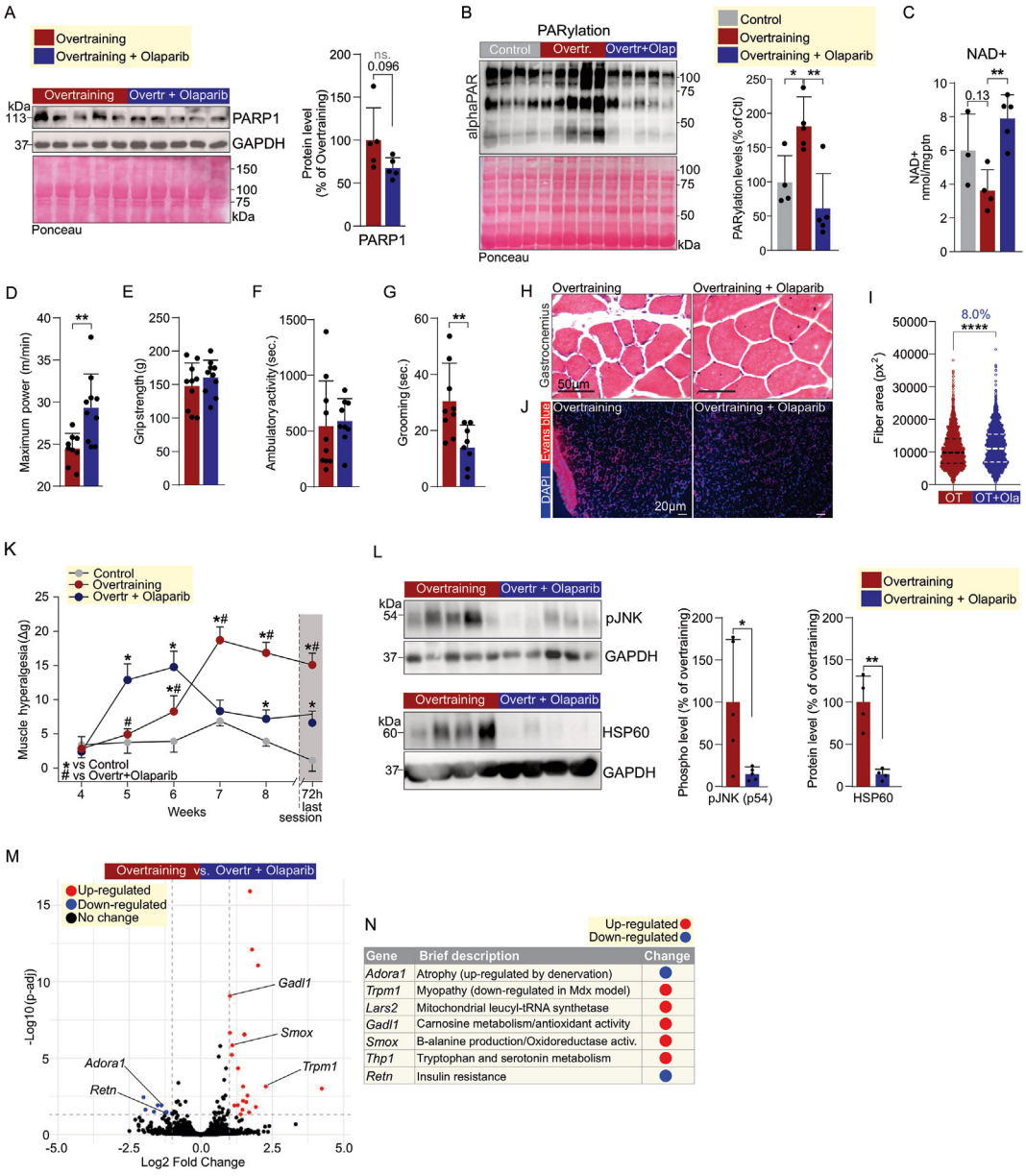

Figure 4: Pharmacological PARP1 inhibition protects against the harmful effects of overtraining in mice. (A) PARP1 protein content (n = 5), (B) Global protein PARylation (n = 4–5), and (C) NAD^+ levels (n = 3–5) in the gastrocnemius muscle of mice treated with Olaparib (50 mg/kg/day). (D) Maximum power (n = 9 and 10). (E) Grip strength (n = 10). (F) Ambulatory activity (n = 9–10) and (G) grooming analysis during the open field test (n = 8–9). (H) Eosin and hematoxylin analysis (n = 5–7). (I) Fiber area measurement (n = 2450). (J) Evans blue staining (red) in gastrocnemius muscle (n = 3). (K) Nociceptive threshold test (n = 5). (L) JNK phosphorylation and HSP60 protein content (n = 5). (M and N) Transcriptome data from skeletal muscle of mice after overtraining versus overtraining plus Olaparib (n = 3). Student's *t*-test was used in A, D, E, F, G, I, and L. Analysis of variance (ANOVA) was used in B, C, and K. *, $p < 0.05$, #, $p < 0.05$, **, $p < 0.01$, ***, $p < 0.001$ and ****, $p < 0.0001$. (For interpretation of the references to color in this figure legend, the reader is referred to the Web version of this article.)

consumer enzyme, we also monitored the intramuscular NAD^+ levels. Olaparib treatment increased NAD^+ accumulation in the skeletal muscle of overtrained mice (Fig. 4C). Together, global protein PARylation and NAD^+ levels confirmed the efficacy of Olaparib treatment in our model.

Olaparib treatment did not affect body weight, fat depots, and muscle weight (Figs. S4A–C). Remarkably, Olaparib-treated mice showed better running capacity during the aerobic power test in overtrained mice (Video 1A). The aerobic performance was enhanced by about 17% when compared to the untreated overtrained group (Fig. 4D). However, no difference was observed in the grip strength (Fig. 4E). Olaparib treatment did not change the locomotor activity pattern (Fig. 4F), but suppressed the stress behavior, as demonstrated by the low grooming pattern immediately after the exercise session (Fig 4G). Supplementary video related to this article can be found at https://doi.org/10.1016/j.molmet.2025.102135

As previously determined (Fig. 2H), overtraining affected the morphology of the muscle fibers (Fig. 4H). Nevertheless, Olaparib treatment preserved the organization of the muscle fibers (Fig. 4H) and increased their size (Fig. 4H and I) compared to untreated overtrained mice. The Evans blue staining demonstrated reduced muscle damage in Olaparib-treated mice (Fig. 4J). These histological findings were

accompanied by reduced muscle hyperalgesia during the last 2 weeks of the overtraining protocol and 72h after the last exercise session in Olaparib-treated mice (Fig. 4K).

Olaparib treatment strongly reduced Jun N-terminal kinase phosphorylation (phospho-JNK) and HSP60 protein content in the skeletal muscle (Fig 4L), indicating that PARP1 inhibition reduced muscle stress, including in the mitochondria. Olaparib increased the protein content of mitochondrial components from complex I (NDUFB8) and complex IV (MTCO1), a protein encoded by the mitochondrial DNA (Fig. S4D). Although Olaparib has positively stimulated the mitochondrial oxygen consumption rate linked to ATP production by 29% and the maximal respiratory capacity by about 15% in the skeletal muscle, no statistical significance was reached (Fig. S4E).

RNAseq analysis revealed that Olaparib modulated 27 genes, including those related to myopathy, atrophy, mitochondrial metabolism, carnosine, beta-alanine and tryptophan production, and insulin resistance in the skeletal muscle of overtrained mice (Fig. 4M, N and S4F). Together, these data reveal that genetic and pharmacological PARP1 inhibition protected muscle fibers against the detrimental effects induced by H_2O_2 in myotubes or overtraining in mice.

3.4. Effects of excessive exercise in the skeletal muscle global PARylation of mice and humans

Beyond overtraining, short periods of excessive exercise may also impact physical performance, potentially leading to muscle damage, stagnation, or reduction in performance [9,39]. This condition can precede both nonfunctional overreaching and overtraining syndrome, affecting up to 30% of regular practitioners of physical activity, including military personnel and athletes [40—42].

Thus, we sought to determine the effects of Olaparib in mice during a short period of excessive training. For this purpose, mice were subjected to 10 consecutive days of treadmill running, which consisted of 3 days of moderate running training (up to 2h or exhaustion), followed by 7 days of excessive training (up to 3h or exhaustion) (Fig .5A). No changes were found in the body weight, as well as the weight of fat, muscle and spleen tissues (Figs. S5A—D). During the moderate training period, both groups gradually improved their performance, reaching the maximum limit of 2 h of training on the third day (Fig. 5B). However, during the excessive exercise period, only a few mice in the vehicle group were able to complete the full 3 h of training. Additionally, these mice presented performance stagnation by the end of the protocol (Fig. 5B). In contrast, all animals in the Olaparib-treated group completed the full 3 h of training in every excessive exercise session (Fig. 5B). The superior performance of the Olaparib-treated group during excessive training can also be seen on video 2 (Video 2). Accumulated exercise time during the excessive exercise period was significantly higher in the Olaparib-treated mice (Fig. 5C). While excessive exercise reduced grip and endurance strengths in the control group, these effects were not observed in the treated group (Figure 5D and E).

Evans blue staining confirmed that the excessive exercise protocol induced skeletal muscle damage and that Olaparib was able to prevent it (Fig. 5F). Olaparib did not change the *Parp1* mRNA levels in the gastrocnemius muscle when compared to vehicle-treated mice (Fig. 5G). Importantly, Olaparib again suppressed the global PARylation levels induced by excessive exercise (Fig. 5H). The pharmacological PARP1 inhibition also prevented excessive exercise-induced JNK phosphorylation and HSP60 accumulation (Fig. 5I), as well as increased the proteins levels of Oxphos-related components (Fig. 5J) in the gastrocnemius muscle.

Finally, muscle samples from healthy subjects who underwent cumulative and progressive high-intensity interval training (HIIT) sessions for 3 weeks [30], were analyzed (Fig 5K). While the number of HIIT sessions increased over the weeks (Fig. 5K), the recovery interval between sessions decreased (Fig. 5L). This protocol reduced glucose tolerance, mitochondrial function, and physical performance at the end of the third week [30]. No changes were observed in the total and cleaved form of PARP1 content in the *vastus lateralis* muscle (Fig 5M). Interestingly, excessive exercise increased the global protein PARylation profile in the skeletal muscle when compared to the basal condition (Fig. 5N). Curiously, the ratio between the physical performance and muscle protein PARylation levels was reduced by excessive exercise (Fig. 5O). Furthermore, excessive exercise also increased HSP60 protein content, a mitostress marker (Fig. 5P). This data aligns with the muscular mitochondrial dysfunction induced in these subjects by the excessive exercise protocol, as previously observed [30]. Together, these findings demonstrate that excessive exercise induces global protein PARylation in both mice and humans and that PARP1 pharmacological inhibition is a promising strategy.

4. DISCUSSION

Typically, drastic reduction or total interruption of the training program are the main recommendations for NFOR and overtraining syndrome prevention [43,44]. Thus, we explored genetic and pharmacological PARP1 inhibition strategies to prevent muscle disorders induced by excessive exercise or overtraining. Recent findings have reported that the proteins of the PARP family are involved in the control of muscle metabolism [11—16] and that high levels of PARP1 and several other PARPs isoforms gene expression were identified in skeletal muscle biopsies from Duchenne muscular dystrophy (DMD) patients [45,46]. In agreement with these human findings, PARP1 activity, and global protein PARylation were also increased in the skeletal muscle of mouse [46], canine [47], models of DMD, and other conditions associated with muscle catabolism, including cancer-cachexia [48,49], and sepsis [50], demonstrating that PARP1 overexpression is intricately linked to the catabolic processes of the skeletal muscle in distinct conditions. Curiously, *Parp1* and *Parp2* genetic deletions protected the skeletal muscle against cancer-induced cachexia in mice [48].

It is important to mention that although PARP1 activity is considered fundamental for DNA repair and other biological processes [18,19], abnormal or aberrant PARP1 activation can trigger detrimental cellular effects, including inflammation, mitochondrial dysfunction, fibrosis, tumor progression, and apoptosis [51—54]. In our study, while adequate exercise programs promoted discrete alterations in the PARylation status of proteins and positive organic adaptations in skeletal muscle, excessive training promoted hyper-PARylation, leading to cellular stress, inflammation, mitochondrial dysfunction, pain, and performance impairment in mice, and mitochondrial stress/dysfunction, metabolic abnormalities, and performance impairment in humans.

In line with our findings, Saini and colleagues also reported that the skeletal muscle PARP1 protein accumulation was negatively associated with aerobic performance during a 6-min walking test in humans [13]. Importantly, oral and intraperitoneal Olaparib treatments were effective and prevented hyper-PARylation induced by excessive training in mice. Furthermore, besides countering the global Parylation promoted by overtraining, it increased the NAD + levels in the skeletal muscle of this model. The increased NAD + levels in the skeletal muscle are directly related to the

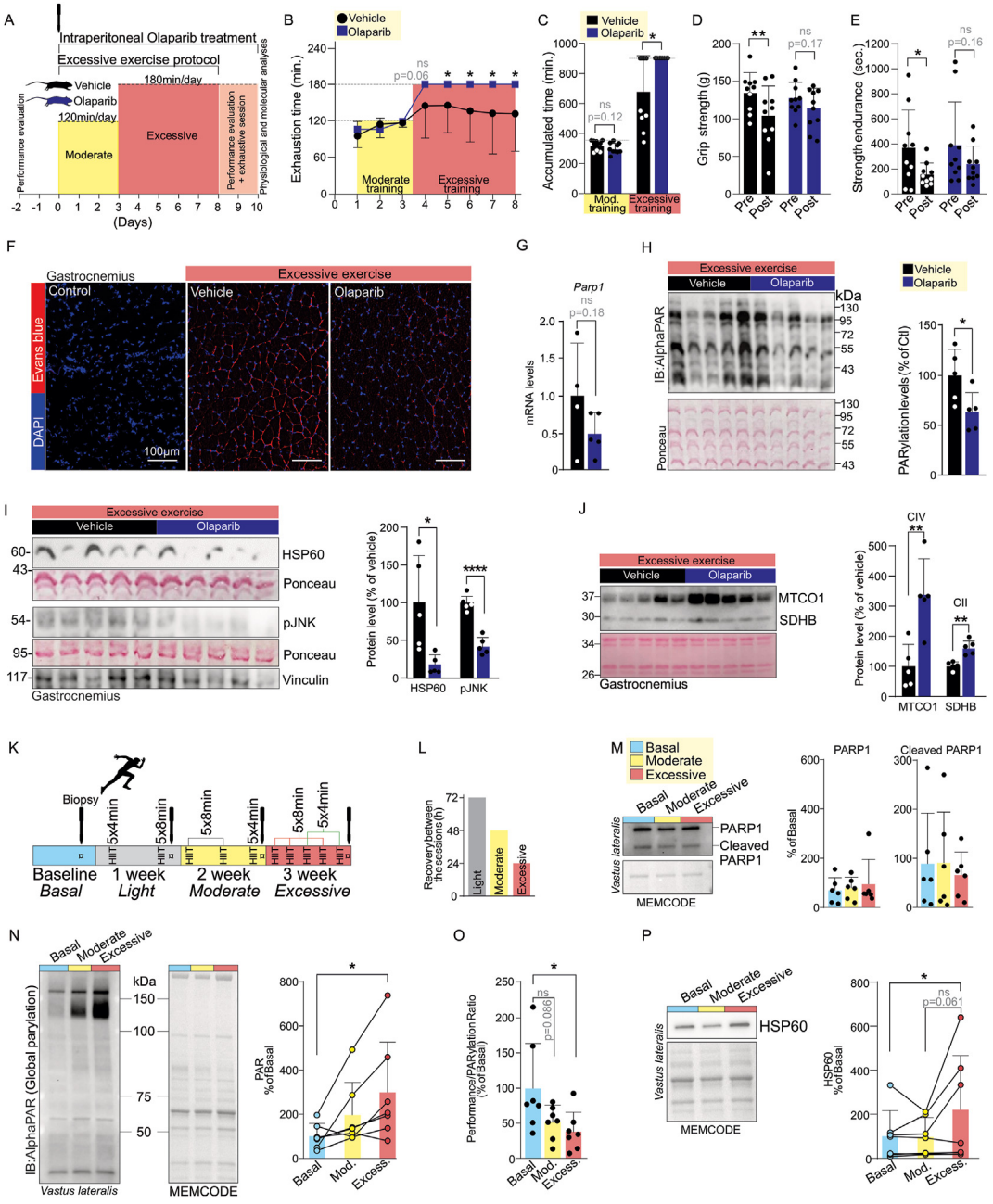

Figure 5: Short-term excessive exercise induces PARylation in mice and humans. (A) Experimental design of the short-term excessive exercise protocol in mice treated with intraperitoneal Olaparib (50 mg/kg/day). (B) Daily exhaustion time (n = 8–10). (C) Accumulated running time (n = 8–10) and (D) Grip strength (n = 10). (E) Strength endurance (n = 10). (F) Evans blue staining (red) in gastrocnemius muscle (n = 4). (G) *Parp1* mRNA levels (n = 4–5), (H) global protein PARylation in muscle (n = 5). (I) JNK phosphorylation and HSP60 protein content (n = 5). (J) OXPHOS-related proteins in muscle (n = 5). (K) Experimental design. (L) Recovery time between HIIT sessions. (M) Cleaved PARP1 (n = 6), (N) global protein PARylation (n = 7). (O) Ratio between maximal heart rate during HIIT sessions and muscle PARylation levels (n = 7). (P) HSP60 protein content (n = 7) in the *vastus lateralis* muscle of healthy subjects. Student's *t*-test was used in B-J. Friedman test was used in N and P. ANOVA was used in other panels. *, $p < 0.05$, **, $p < 0.01$, ***, $p < 0.001$ and ****, $p < 0.0001$. (For interpretation of the references to color in this figure legend, the reader is referred to the Web version of this article.)

improvement of muscle function in a DMD model [46]. Previously, Olaparib also proved itself as a potential drug for the treatment of metabolic diseases [16]. Based on these observations, Olaparib and other PARP inhibitors currently available for cancer treatment could be repropose for the treatment of myopathies and metabolic diseases. Thus, pharmacological or nutritional strategies aimed at reducing the hyper-PARylation of muscle proteins appear to be promising for preventing or treating symptoms of overtraining.

PARP1 is recognized as a DNA-dependent enzyme [55–58] and it is activated by distinct DNA structures such as single- or double-strand DNA breaks, R-loops, cruciform, and hairpin DNAs [59–62]. The precise mechanism by which excessive exercise provoked PARP1 activation was not investigated in the present study. However, we previously demonstrated that overtraining induced DNA damage in the skeletal muscle of mice [37]. A meta-analysis study has reported that muscle contraction induced by exercise triggers significant DNA

damage in the muscle fibers of humans [63], suggesting that mechanical and/or oxidative stress may be a determinant for PARP1 activation in response to exercise. Consistent with this, excessive mechanical stress-induced DNA damage, elicited PARP1 activity and reduced intracellular NAD + levels in C2C12 cells and the skeletal muscle of mice [64]. In addition, chronic atrial fibrillation induced by intermittent optogenetic tachypacing also induces DNA damage, NAD + depletion, and strong PARP activation in cardiomyocytes [14]. Importantly, we demonstrated that repeated muscle contractions resulting from an adequate exercise program did not affect PARP1 activity and were able to promote positive organic adaptations in skeletal muscle, suggesting that PARP1 activation occurs only in an overcompensated exercise program.

It is important to emphasize that acute fatigue represents a transient physiological state characterized by reversible metabolic disturbances such as metabolite accumulation, electrolyte imbalance, acute inflammation, and typically rapid recovery. In contrast, overtraining is a maladaptive response to prolonged excessive training load, involving persistent alterations such as chronic inflammation, sustained oxidative stress, mitochondrial dysfunction, and hormonal imbalances, which collectively require extended periods for recovery [5,65,66]. Notably, in our short-term excessive exercise protocol, pharmacological inhibition of PARP1 with Olaparib improved aerobic performance from the fifth to the eighth day (Fig. 5B) compared to untreated animals. This finding suggests that PARP1 inhibition may acutely or rapidly enhance aerobic performance; however, this hypothesis was not directly addressed in the present study and warrants further investigation.

PARP1 is responsible for about 90% of PARylation of the intracellular proteins [19], but the mechanism by which aberrant PARP1 activation can affect muscle function and physical performance is unclear. PARP1 activation controls the key proteins related to muscle bioenergetics and contraction, including NRF1 [67] and AMPK [15]. For instance, PARP1 activation reduces AMPK phosphorylation through a PARylation-dependent mechanism, affecting muscle contraction capacity in *Drosophila* [15]. Furthermore, PARP1 activation requires NAD^+ consumption, limiting Sirt1 deacetylase activity, leading to acetylation and inhibition of the master regulator of muscle metabolism, PGC1-α [12,14,23,47,68,69]. PARP1 activation also promotes fibrosis [54] and a wide chromatin remodeling [70,71], which may affect muscle contraction capacity. Conversely, PARP1 inhibition or NAD^+ repletion improves mitochondrial function and muscle performance in *C. elegans* and mice [16,27,46].

Thus, the results presented in this report not only offer novel biological insight into the aberrant PARP1 activity associated with skeletal muscle abnormalities in response to excessive exercise but also propose PARP1 as a critical target for preventing the NFOR state and overtraining syndrome.

5. LIMITATIONS OF THE STUDY

While pharmacological inhibition of PARP1 has demonstrated beneficial effects on the muscles of overtrained mice, the current study did not evaluate the effects of Olaparib on the muscle regeneration process. The investigation of pathways how Olaparib affects the muscle regeneration process would better determine the drug application as an off-lab drug for different muscle conditions, for example, myopathies. Comparing the present data with other models of muscle damage (myopathies, induced damage) would increase our understanding of its actions. Furthermore, no specific target of PARP1 was identified in this report. It is plausible that multiple substrates can undergo MARylation or PARylation to control the different cellular processes evaluated. Importantly, since Olaparib improved performance not only in the overtrained model but also in the excessive exercise short protocol, we did not investigate whether hyperPARylation is a consequence of an acute fatigue state or related to the overtraining process, which requires further investigation. Finally, it is important to consider that although Olaparib has been used successfully in mice, this drug is considered off-label for this purpose in humans.

ACKNOWLEDGMENTS

This work was supported by grants from the São Paulo Research Foundation (FAPESP- 2013/07607-8, 2018/04192-5, 2019/21709-4, 2019/22512-0, 2021/08354-2, 2022/08930-6). Brazilian National Council for Scientific and Technological Development - CNPq (304123/2023-4 and 309268/2023-0) and Coordination for the Improvement of Higher Education Personnel (CAPES), number 001. The authors would like to acknowledge the MyoImage Platform from the UMR974, Institut de Myologie, particularly Zoheir Guesmia, for help with fiber size analysis. The authors thank the Obesity and Comorbidities Research Center (OCRC) and prof. Licio A. Velloso for RNAseq experiment.

DECLARATION OF GENERATIVE AI AND AI-ASSISTED TECHNOLOGIES

No AI-assisted technologies were used to write this manuscript, except for the reference editing tool.

CRediT AUTHORSHIP CONTRIBUTION STATEMENT

Barbara M. Crisol: Formal analysis, Data curation. **Matheus B. Rocha:** Formal analysis, Data curation. **Beatriz Franco:** Formal analysis, Data curation. **Ana Paula Morelli:** Formal analysis, Data curation. **Carlos K. Katashima:** Formal analysis, Data curation. **Scylas J.A. Junior:** Formal analysis, Data curation. **Fernanda S. Carneiro:** Formal analysis, Data curation. **Renata R. Braga:** Data curation. **Rafael S. Brícola:** Data curation. **Graciana de Azambuja:** Formal analysis, Data curation. **Raul Gobato Costa:** Methodology, Formal analysis, Data curation. **Andrea M. Esteves:** Writing — review & editing. **Marcelo A. Mori:** Writing — review & editing. **Maria C.G. Oliveira:** Writing — review & editing. **Dennys E. Cintra:** Writing — review & editing. **José R. Pauli:** Writing — review & editing. **Filip J. Larsen:** Writing — review & editing. **Adelino S.R. da Silva:** Writing — review & editing, Visualization. **Eduardo R. Ropelle:** Writing — review & editing, Supervision, Funding acquisition, Conceptualization.

DECLARATION OF COMPETING INTEREST

The authors declare that they have no known competing financial interests or personal relationships that could have appeared to influence the work reported in this paper.

DATA AVAILABILITY

Data will be made available on request.

APPENDIX A. SUPPLEMENTARY DATA

Supplementary data to this article can be found online at https://doi.org/10.1016/j.molmet.2025.102135.

REFERENCES

[1] Carrard J, Rigort AC, Appenzeller-Herzog C, Colledge F, Königstein K, Hinrichs T, et al. Diagnosing overtraining syndrome: a scoping review. Sport Health 2022. https://doi.org/10.1177/19417381211044739.

[2] Armstrong LE, Bergeron MF, Lee EC, Mershon JE, Armstrong EM. Overtraining syndrome as a complex systems phenomenon. Frontiers in Network Physiology 2021. https://doi.org/10.3389/fnetp.2021.794392.

[3] Weakley J, Halson SL, Mujika I. Overtraining syndrome symptoms and diagnosis in athletes: where is the research? A systematic review. Int J Sports Physiol Perform 2022. https://doi.org/10.1123/ijspp.2021-0448.

[4] Buyse L, Decroix L, Timmermans N, Barbé K, Verrelst R, Meeusen R. Improving the diagnosis of nonfunctional overreaching and overtraining syndrome. Med Sci Sports Exerc 2019;51(12):2524–30. https://doi.org/10.1249/MSS.0000000000002084.

[5] Cheng AJ, Jude B, Lanner JT. Intramuscular mechanisms of overtraining. Redox Biol 2020. https://doi.org/10.1016/j.redox.2020.101480.

[6] Marafon BB, Pinto AP, Ropelle ER, de Moura LP, Cintra DE, Pauli JR, et al. Muscle endoplasmic reticulum stress in exercise. Acta Physiol 2022. https://doi.org/10.1111/apha.13799.

[7] Gandra PG, Valente RH, Perales J, Pacheco AGF, Macedo DV. Proteomic profiling of skeletal muscle in an animal model of overtraining. Proteomics 2012;12(17):2663–7. https://doi.org/10.1002/PMIC.201200137.

[8] da Rocha AL, Pereira BC, Teixeira GR, Pinto AP, Frantz FG, Elias LLK, et al. Treadmill slope modulates inflammation, fiber type composition, androgen, and glucocorticoid receptors in the skeletal muscle of overtrained mice. Front Immunol 2017;8. https://doi.org/10.3389/fimmu.2017.01378. OCT.

[9] Pereira BC, Pauli JR, De Souza CT, Ropelle ER, Cintra DE, Rocha EM, et al. Nonfunctional overreaching leads to inflammation and myostatin upregulation in swiss mice. Int J Sports Med 2014;35(2). https://doi.org/10.1055/s-0033-1349077.

[10] Snyder AC. Overtraining and glycogen depletion hypothesis. Med Sci Sports Exerc 1998;30.

[11] Matteini F, Andresini O, Petrai S, Battistelli C, Rossi MN, Maione R. Poly(ADP-ribose) Polymerase 1 (PARP1) restrains MyoD-dependent gene expression during muscle differentiation. Sci Rep 2020;10(1). https://doi.org/10.1038/s41598-020-72155-8.

[12] Mohamed JS, Wilson JC, Myers MJ, Sisson KJ, Alway SE. Dysregulation of SIRT-1 in aging mice increases skeletal muscle fatigue by a PARP-1-dependent mechanism. Aging 2014;6(10). https://doi.org/10.18632/aging.100696.

[13] Saini SK, Li L, Peek CB, Kosmac K, Polonsky TS, Tian L, et al. Associations of Poly (ADP-Ribose) Polymerase1 abundance in calf skeletal muscle with walking performance in peripheral artery disease. Exp Gerontol 2020;140. https://doi.org/10.1016/j.exger.2020.111048.

[14] Zhang D, Hu X, Li J, Liu J, Baks-te Bulte L, Wiersma M, et al. DNA damage-induced PARP1 activation confers cardiomyocyte dysfunction through NAD + depletion in experimental atrial fibrillation. Nat Commun 2019;10(1). https://doi.org/10.1038/s41467-019-09014-2.

[15] Guo S, Zhang S, Zhuang Y, Xie F, Wang R, Kong X, et al. Muscle PARP1 inhibition extends lifespan through AMPKα PARylation and activation in Drosophila. Proc Natl Acad Sci USA 2023;120(13). https://doi.org/10.1073/pnas.2213857120.

[16] Pirinen E, Cantó C, Jo YS, Morato L, Zhang H, Menzies KJ, et al. Pharmacological inhibition of poly(ADP-ribose) polymerases improves fitness and mitochondrial function in skeletal muscle. Cell Metab 2014;19(6). https://doi.org/10.1016/j.cmet.2014.04.002.

[17] Serrano J, Boyd J, Brown IS, Mason C, Smith KR, Karolyi K, et al. The TAS1R2 G-protein-coupled receptor is an ambient glucose sensor in skeletal muscle that regulates NAD homeostasis and mitochondrial capacity. Nat Commun 2024;15(1). https://doi.org/10.1038/S41467-024-49100-8.

[18] Suskiewicz MJ, Prokhorova E, Rack JGM, Ahel I. ADP-ribosylation from molecular mechanisms to therapeutic implications. Cell 2023. https://doi.org/10.1016/j.cell.2023.08.030.

[19] Tallis M, Morra R, Barkauskaite E, Ahel I. Poly(ADP-ribosyl)ation in regulation of chromatin structure and the DNA damage response. Chromosoma 2014. https://doi.org/10.1007/s00412-013-0442-9.

[20] Ferreira JCB, Rolim NPL, Bartholomeu JB, Gobatto CA, Kokubun E, Brum PC. Maximal lactate steady state in running mice: effect of exercise training. Clin Exp Pharmacol Physiol 2007;34(8):760–5. https://doi.org/10.1111/j.1440-1681.2007.04635.x.

[21] Pereira BC, Filho LAL, Alves GF, Pauli JR, Ropelle ER, Souza CT, et al. A new overtraining protocol for mice based on downhill running sessions. Clin Exp Pharmacol Physiol 2012;39(9). https://doi.org/10.1111/j.1440-1681.2012.05728.x.

[22] Deacon RMJ. Measuring the strength of mice. J Vis Exp 2013;(76). https://doi.org/10.3791/2610.

[23] Gariani K, Ryu D, Menzies KJ, Yi H-S, Stein S, Zhang H, et al. Inhibiting poly ADP-ribosylation increases fatty acid oxidation and protects against fatty liver disease. J Hepatol 2017;66(1):132–41. https://doi.org/10.1016/j.jhep.2016.08.024.

[24] de Azambuja G, Jorge CO, Gomes BB, Lourenço HR, Simabuco FM, Oliveira-Fusaro MCG. Regular swimming exercise prevented the acute and persistent mechanical muscle hyperalgesia by modulation of macrophages phenotypes and inflammatory cytokines via PPARγ receptors. Brain Behav Immun 2021;95:462–76. https://doi.org/10.1016/J.BBI.2021.05.002.

[25] Hamer PW, McGeachie JM, Davies MJ, Grounds MD. Evans Blue Dye as an in vivo marker of myofibre damage: optimising parameters for detecting initial myofibre membrane permeability. J Anat 2002;200:69–79. https://doi.org/10.1046/J.0021-8782.2001.00008.X. Pt 1.

[26] Cantó C, Garcia-Roves PM. High-resolution respirometry for mitochondrial characterization of ex vivo mouse tissues. Curr Protoc Mol Biol 2015;5(2):135–53. https://doi.org/10.1002/9780470942390.MO140061.

[27] Crisol BM, Veiga CB, Braga RR, Lenhare L, Baptista IL, Gaspar RC, et al. NAD+ precursor increases aerobic performance in mice. Eur J Nutr 2019. https://doi.org/10.1007/s00394-019-02089-z.

[28] Bankhead P, Loughrey MB, Fernández JA, Dombrowski Y, McArt DG, Dunne PD, et al. QuPath: open source software for digital pathology image analysis. Scientific Reports 2017 2017;7(1):1–7. https://doi.org/10.1038/s41598-017-17204-5. 1 7.

[29] Kanamori KS, de Oliveira GC, Auxiliadora-Martins M, Schoon RA, Reid JM, Chini EN. Two different methods of quantification of oxidized nicotinamide adenine dinucleotide (NAD+) and reduced nicotinamide adenine dinucleotide (NADH) intracellular levels: enzymatic coupled cycling assay and ultra-performance liquid chromatography (UPLC)-Mass spectrometry. Bio-Protocol 2018;8(14). https://doi.org/10.21769/BioProtoc.2937.

[30] Flockhart M, Nilsson LC, Tais S, Ekblom B, Apró W, Larsen FJ. Excessive exercise training causes mitochondrial functional impairment and decreases glucose tolerance in healthy volunteers. Cell Metab 2021;33(5). https://doi.org/10.1016/j.cmet.2021.02.017.

[31] Williams EG, Wu Y, Jha P, Dubuis S, Blattmann P, Argmann CA, et al. Systems proteomics of liver mitochondria function. Science 2016;352(6291):aad0189. https://doi.org/10.1126/science.aad0189. aad0189.

[32] Li X, Morel JD, Sulc J, De Masi A, Lalou A, Benegiamo G, et al. Systems genetics of metabolic health in the BXD mouse genetic reference population. Cell Systems 2024;15(6):497–509.e3. https://doi.org/10.1016/J.CELS.2024.05.006.

[33] Koshiba S, Motoike IN, Saigusa D, Inoue J, Aoki Y, Tadaka S, et al. Identification of critical genetic variants associated with metabolic phenotypes of the Japanese population. Commun Biol 2020;3(1). https://doi.org/10.1038/s42003-020-01383-5.

[34] Schulz P, Jansseune K, Degenkolbe T, Meret M, Claeys H, Skirycz A, et al. Poly(ADP-Ribose)polymerase activity controls plant growth by promoting leaf cell number. PLoS One 2014;9(2). https://doi.org/10.1371/journal.pone.0090322.

[35] da Rocha ALAL, Pereira BCBC, Pauli JRJR, de Souza CTCT, Teixeira GRGR, Lira FSFS, et al. Downhill running excessive training inhibits hypertrophy in mice skeletal muscles with different fiber type composition. J Cell Physiol 2016;231(5):1045–56. https://doi.org/10.1002/jcp.25197.

[36] Morais GP, da Rocha AL, Neave LM, de A, Lucas G, Leonard TR, et al. Chronic uphill and downhill exercise protocols do not lead to sarcomerogenesis in mouse skeletal muscle. J Biomech 2020;98. https://doi.org/10.1016/J.JBIOMECH.2019.109469.

[37] Pereira BBC, Pauli JJR, Antunes LMLMG, De Freitas EEC, De Almeida M, De Paula Venâncio V, et al. Overtraining is associated with DNA damage in blood and skeletal muscle cells of Swiss mice. BMC Physiol 2013;13(1):11. https://doi.org/10.1186/1472-6793-13-11.

[38] Zhen Y, Yu Y. Proteomic analysis of the downstream signaling network of PARP1. Biochemistry 2018. https://doi.org/10.1021/acs.biochem.7b01022.

[39] Bell L, Ruddock A, Maden-Wilkinson T, Rogerson D. Overreaching and overtraining in strength sports and resistance training: a scoping review. J Sports Sci 2020;38(16). https://doi.org/10.1080/02640414.2020.1763077.

[40] Williams CA, Winsley RJ, Pinho G, De M, Croix S, Lloyd RS, et al. Prevalence of non-functional overreaching in elite male and female youth academy football players. Science and Medicine in Football 2017;1(3):222–8. https://doi.org/10.1080/24733938.2017.1336282.

[41] Tanskanen MM, Kyröläinen H, Uusitalo AL, Huovinen J, Nissilä J, Kinnunen H, et al. Serum sex hormone-binding globulin and cortisol concentrations are associated with overreaching during strenuous military training. J Strength Condit Res 2011;25(3). https://doi.org/10.1519/JSC.0b013e3181c1fa5d.

[42] Tian Y, He Z, Zhao J, Tao D, Xu K, Midgley A, et al. An 8-year longitudinal study of overreaching in 114 elite female Chinese wrestlers. J Athl Train 2015;50(2):217–23. https://doi.org/10.4085/1062-6050-49.3.57.

[43] Meeusen R, Duclos M, Foster C, Fry A, Gleeson M, Nieman D, et al. Prevention, diagnosis, and treatment of the overtraining syndrome: joint consensus statement of the european college of sport science and the American College of Sports Medicine. Med Sci Sports Exerc 2013;45(1). https://doi.org/10.1249/MSS.0b013e318279a10a.

[44] Prevention, diagnosis, and treatment of the overtraining syndrome. Med Sci Sports Exerc 2013;45(1). https://doi.org/10.1249/mss.0b013e318279a10a.

[45] Aguennouz M, Vita GL, Messina S, Cama A, Lanzano N, Ciranni A, et al. Telomere shortening is associated to TRF1 and PARP1 overexpression in Duchenne muscular dystrophy. Neurobiol Aging 2011;32(12). https://doi.org/10.1016/j.neurobiolaging.2010.01.008.

[46] Ryu D, Zhang H, Ropelle ER, Sorrentino V, Mázala DAG, Mouchiroud L, et al. NAD+ repletion improves muscle function in muscular dystrophy and counters global parylation. Sci Transl Med 2016;8(361). https://doi.org/10.1126/scitranslmed.aaf5504.

[47] Cardoso D, Barthélémy I, Blot S, Muchir A. Replenishing NAD+ content reduces aspects of striated muscle disease in a dog model of Duchenne muscular dystrophy. Skeletal Muscle 2023;13(1). https://doi.org/10.1186/s13395-023-00328-w.

[48] Chacon-Cabrera A, Fermoselle C, Salmela I, Yelamos J, Barreiro E. MicroRNA expression and protein acetylation pattern in respiratory and limb muscles of Parp-1-/- and Parp-2-/- mice with lung cancer cachexia. Biochim Biophys Acta Gen Subj 2015;1850(12). https://doi.org/10.1016/j.bbagen.2015.09.020.

[49] Chacon-Cabrera A, Mateu-Jimenez M, Langohr K, Fermoselle C, García-Arumí E, Andreu AL, et al. Role of PARP activity in lung cancer-induced cachexia: effects on muscle oxidative stress, proteolysis, anabolic markers, and phenotype. J Cell Physiol 2017;232(12). https://doi.org/10.1002/jcp.25851.

[50] Santos SS, Brunialti MKC, Soriano FG, Szabo C, Salomão R. Repurposing of clinically approved poly-(ADP-ribose) polymerase inhibitors for the therapy of sepsis. Shock 2021. https://doi.org/10.1097/SHK.0000000000001820.

[51] Kumar V, Kumar A, Mir KUl, Yadav V, Chauhan SS. Pleiotropic role of PARP1: an overview. 3 Biotech 2022. https://doi.org/10.1007/s13205-021-03038-6.

[52] Huang D, Kraus WL. The expanding universe of PARP1-mediated molecular and therapeutic mechanisms. Mol Cell 2022;82(12):2315–34. https://doi.org/10.1016/J.MOLCEL.2022.02.021.

[53] Ma Z, Feng D, Rui W, Wang Z. Baicalin attenuates chronic unpredictable mild stress-induced hippocampal neuronal apoptosis through regulating SIRT1/PARP1 signaling pathway. Behav Brain Res 2023;441. https://doi.org/10.1016/J.BBR.2023.114299.

[54] Sun S, Hu Y, Zheng Q, Guo Z, Sun D, Chen S, et al. Poly(ADP-ribose) polymerase 1 induces cardiac fibrosis by mediating mammalian target of rapamycin activity. J Cell Biochem 2019;120(4):4813–26. https://doi.org/10.1002/JCB.26649.

[55] Petropoulos M, Karamichali A, Rossetti GG, Freudenmann A, Iacovino LG, Dionellis VS, et al. Transcription-replication conflicts underlie sensitivity to PARP inhibitors. Nature 2024;628(8007):433–41. https://doi.org/10.1038/S41586-024-07217-2.

[56] Fried W, Tyagi M, Minakhin L, Chandramouly G, Tredinnick T, Ramanjulu M, et al. Discovery of a small-molecule inhibitor that traps Polθ on DNA and synergizes with PARP inhibitors. Nat Commun 2024;15(1). https://doi.org/10.1038/S41467-024-46593-1.

[57] Langelier MF, Planck JL, Roy S, Pascal JM. Structural basis for DNA damage-dependent poly(ADP-ribosyl)ation by human PARP-1. Science 2012;336(6082). https://doi.org/10.1126/science.1216338.

[58] Chambon P, Weill JD, Mandel P. Nicotinamide mononucleotide activation of a new DNA-dependent polyadenylic acid synthesizing nuclear enzyme. Biochem Biophys Res Commun 1963;11(1). https://doi.org/10.1016/0006-291X(63)90024-X.

[59] Lonskaya I, Potaman VN, Shlyakhtenko LS, Oussatcheva EA, Lyubchenko YL, Soldatenkov VA. Regulation of poly(ADP-ribose) polymerase-1 by DNA structure-specific binding. J Biol Chem 2005;280(17). https://doi.org/10.1074/jbc.M413483200.

[60] Laspata N, Muoio D, Fouquerel E. Multifaceted role of PARP1 in maintaining genome stability through its binding to alternative DNA structures. J Mol Biol 2024. https://doi.org/10.1016/j.jmb.2023.168207.

[61] van Beek L, McClay É, Patel S, Schimpl M, Spagnolo L, Maia de Oliveira T. Parp power: a structural perspective on parp1, parp2, and parp3 in dna damage repair and nucleosome remodelling. Int J Mol Sci 2021. https://doi.org/10.3390/ijms22105112.

[62] Bell NAW, Molloy JE. Single-molecule force spectroscopy reveals binding and bridging dynamics of PARP1 and PARP2 at DNA double-strand breaks. Proc Natl Acad Sci USA 2023;120(22). https://doi.org/10.1073/pnas.2214209120.

[63] Tryfidou DV, McClean C, Nikolaidis MG, Davison GW. DNA damage following acute aerobic exercise: a systematic review and meta-analysis. Sports Med 2020. https://doi.org/10.1007/s40279-019-01181-y.

[64] Huang G, He Y, Hong L, Zhou M, Zuo X, Zhao Z. Restoration of NAD+ homeostasis protects C2C12 myoblasts and mouse levator ani muscle from mechanical stress-induced damage. Anim Cell Syst 2022;26(4). https://doi.org/10.1080/19768354.2022.2106303.

[65] Watanabe D, Wada M. Cellular mechanisms underlying overreaching in skeletal muscle following excessive high-intensity interval training. Am J Physiol Cell Physiol 2025;328(3):C921–38. https://doi.org/10.1152/AJPCELL.00623.2024.

[66] Roussel OP, Pignanelli C, Hubbard EF, Coates AM, Cheng A, Burr JF, et al. Effects of intensified training with insufficient recovery on joint level and single muscle fibre mechanical function: the role of myofibrillar Ca2+ sensitivity. Applied Physiology, Nutrition, and Metabolism = Physiologie Appliquee, Nutrition et Metabolisme 2024;49(12). https://doi.org/10.1139/APNM-2024-0189.

[67] Hossain MB, Ji P, Anish R, Jacobson RH, Takada S. Poly(ADP-ribose) polymerase 1 interacts with nuclear respiratory factor 1 (NRF-1) and plays a role in NRF-1 transcriptional regulation. J Biol Chem 2009;284(13). https://doi.org/10.1074/jbc.M807198200.

[68] Bai P, Cantó C, Oudart H, Brunyánszki A, Cen Y, Thomas C, et al. PARP-1 inhibition increases mitochondrial metabolism through SIRT1 activation. Cell Metab 2011;13(4). https://doi.org/10.1016/j.cmet.2011.03.004.

[69] Scheibye-Knudsen M, Mitchell SJ, Fang EF, Iyama T, Ward T, Wang J, et al. A high-fat diet and NAD+ activate sirt1 to rescue premature aging in cockayne syndrome. Cell Metab 2014;20(5). https://doi.org/10.1016/j.cmet.2014.10.005.

[70] Kang M, Park S, Park SH, Lee HG, Park JH. A double-edged sword: the two faces of PARylation. Int J Mol Sci 2022. https://doi.org/10.3390/ijms23179826.

[71] Safdar R, Mishra A, Shah GM, Ashraf MZ. Poly (ADP-ribose) Polymerase-1 modulations in the genesis of thrombosis. J Thromb Thrombolysis 2024;57(5):743–53. https://doi.org/10.1007/S11239-024-02974-3.

